

6th International Conference on Creep, Fatigue and Creep-Fatigue Interaction [CF-6]

Creep-induced Microstructural Changes in Large Welded Joints of High Cr Heat Resistant Steel

Yuta Tanaka^{*}, Keiji Kubushiro, Satoshi Takahashi,
Noriko Saito, Hirokatsu Nakagawa

IHI Corporation, 1, Shin-Nakahara-cho, Isogo-ku, Yokohama, 235-8501, Japan

Abstract

The creep damage process of high-Cr steel welded joints is characterized by the formation and growth of creep voids prior to the initiation of cracking, and this formation and growth accounts for a large proportion of creep life. Therefore, there has been much investigation into the detection and quantitative evaluation of creep voids and microcracks in welded joints for use in remaining life assessment. However, the microstructure around creep voids and microcracks is still not well known. In this study, a creep test on a large welded joint in Mod.9Cr-1Mo steel was conducted under 60 MPa at 650°C. The observation of the microstructure in the heat-affected zone (HAZ) was made for the specimen interrupted the creep tests at 25% of a rupture life. The microstructure around the creep void was characterized using an electron backscatter diffraction pattern (EBSD) method. It was founded that creep voids formed and developed along random high angle grain boundaries that were not subject to K-S orientation relationship in the martensitic transformation. In addition, the initially formed void promoted preferential dynamic recovery and dynamic recrystallization in its surrounding microstructure, followed by sub-boundary formation.

© 2013 The Authors. Published by Elsevier Ltd. Open access under [CC BY-NC-ND license](#).
Selection and peer-review under responsibility of the Indira Gandhi Centre for Atomic Research.

Keywords: Mod.9Cr-1Mo steel; creep voids; damage assessment; EBSD, sub-boundary

1. Introduction

Mod.9Cr-1Mo steel has been widely used for high-temperature structures such as boiler components in ultra-supercritical (USC) thermal power plants. These materials have attained high creep strength due to their having a tempered martensitic structure with a high dislocation density and an internal block/lath structure formed of prior austenite grains and fine carbide precipitation. However, it was reported that the creep strength of welded joints in high Cr steels is significantly lower than that in the case of base metals [1]. Creep damage in the welded joint preferentially accumulated in the fine-grained HAZ. As a result, so-called Type IV fractures occur.

^{*} Corresponding author:
E-mail address: yuta_tanaka@ihi.co.jp

At the same time, studies of the assessment of creep damage and the mechanisms of Type IV fracture have been investigated, based on mechanical and microstructural approaches. It has been computed using the finite element method analysis that complex multiaxial stress distributed in the welded joint affects the creep damage process in HAZ [2]. Meanwhile, it has been proposed that the void formation at grain boundaries was caused by strain heterogeneity among grains, and the growth of voids was assisted by the creep strain concerned in HAZ, based on microstructure observations of Mod.9Cr-1Mo steel welded joints [3]. However, the creep damage process in Mod.9Cr-1Mo steel welded joints is not fully understood based on this detailed microstructural assessment.

Recently, the EBSD pattern method, which enables mapping of crystal orientation as a function of position, has been successfully applied to investigate crystallographic morphologies. In this study, the Type IV creep damage process using large and thick welded joints in Mod.9Cr-1Mo steel was investigated. The relationship between the sites where the creep voids and microcracking were initiated and the microstructural changes was evaluated using an EBSD system incorporating an SEM (SEM/EBSD).

2. Experimental procedures

The material investigated in the present study is a 60 mm-thick Mod.9Cr-1Mo steel plate. The plate was welded using a shielded metal arc welding process. Post weld heat treatment (PWHT) was conducted at 740°C for 2 hours. A creep test of the large welded joint in Mod.9Cr-1Mo steel was conducted under 60 MPa at 650°C, and the creep test were interrupted at 25% of a rupture life in order to investigate the damage process.

An EBSD analysis was conducted in an FE-SEM with the specimen tilted by 70° after polishing with colloidal silica. The area selected for EBSD analysis was 50 μm^2 with a step size of 25 nm. In this study, the EBSD images are represented either as image quality (IQ) maps or as inverse pole figure (IPF) maps. The IQ maps represent the quality of EBSD patterns and can be used to approximate the relative presence of a strain in a deformed microstructure. Meanwhile, the IPF maps show the crystallographic orientations using suitable color codes.

3. Results and discussion

3.1. Characterization of HAZ microstructure using EBSD

The microstructural observation of welded joint without creep was evaluated using EBSD analysis. Figure 1 shows the IQ map (misorientation $>5^\circ$) in (a) base metal before PWHT, (b) 0.5 mm from bond line (equivalent to coarse-grained HAZ) before PWHT, (c) 2.0 mm from bond line (equivalent to fine-grained HAZ) before PWHT, and (d) 2.0 mm from bond line after PWHT. The base metal was typically tempered martensite dominated by linear block boundaries at a rotation angle of 60° (the gray lines in Fig. 1). In the case of HAZ near the bond line (such as Fig. 1(b)), large grains and linear block boundaries similar to those in base metal were observed due to the tempered martensite being heated into γ single-phase field. In contrast, many smaller grains were observed in the fine-grained HAZ. These grains are consistent with γ nucleation due to rapid heating into the $(\alpha + \gamma)$ phase field during the weld thermal cycle. The ratio of the small grains decreased due to recovery during PWHT, as shown in Fig. 1(d). This microstructural changes indicates that fine-grained HAZ is an unstable microstructure that has a tendency to cause recovery and crystallization.

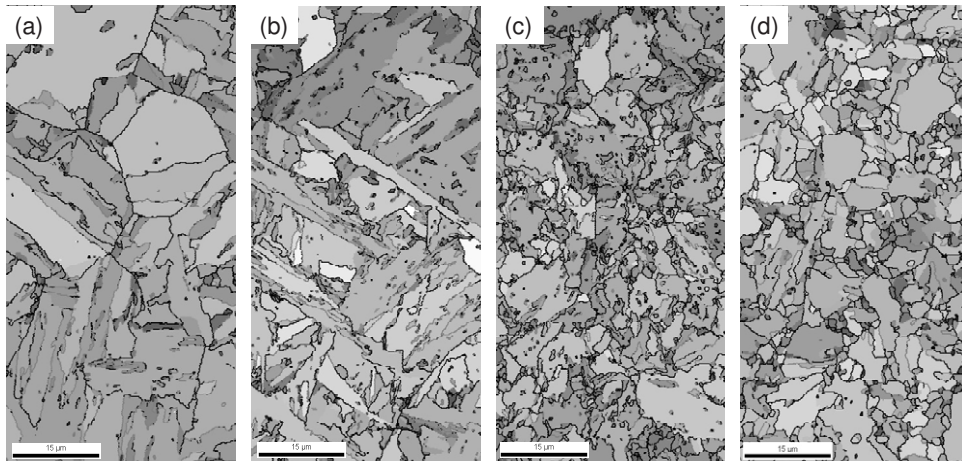


Fig. 1. EBSD IQ map in (a) base metal before PWHT, (b) 0.5 mm from bond line before PWHT, (c) 2.0 mm from bond line before PWHT, and (d) 2.0 mm from bond line after PWHT. Gray line shows block boundaries with rotation angle of 60° .

3.2. Characterization of microstructure around creep voids in HAZ

Creep voids (including microcracks) were observed on/along grain boundaries in both (a–c) coarse-grained HAZ and (d–f) fine-grained HAZ in Fig. 2 and their size as observed using SEM was approximately $1\ \mu\text{m}$. The proportion of the area accounted for by these creep voids throughout HAZ was larger in fine-grained HAZ than in coarse-grained HAZ. The sites of the initiation of creep voids were at the triple junction of prior austenite boundaries (the dashed line in Fig. 2(b)) in coarse-grained HAZ, but this was not necessarily the case in fine-grained HAZ. In addition, precipitates such as Laves phase and M_{23}C_6 were randomly distributed regardless of whether creep voids were present or not. This suggested that they play no role in the initiation of creep voids.

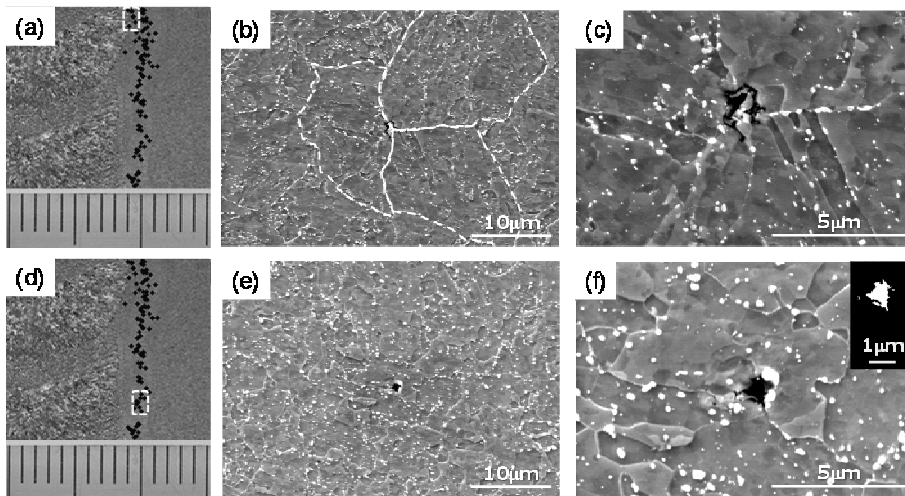


Fig. 2. Creep voids distribution for the creep specimen interrupted at 25% of a rupture life (a, d). Creep voids are on grain boundaries in both coarse-grained HAZ (b, c) and fine-grained HAZ (e, f).

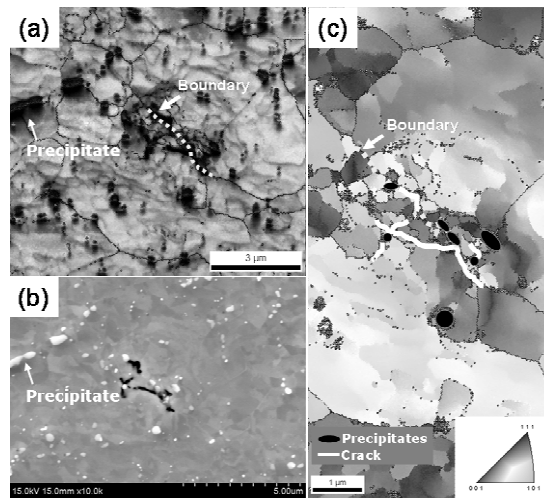


Fig. 3. Creep voids (microcracks) in fine-grained HAZ for the specimen interrupted the creep test at 25% of a rupture life: (a) IQ map, (b) SEM image, and (c) IPF map.

The creep voids were surrounded with layers of very fine grains of less than $1\ \mu\text{m}$, as shown in Fig. 3(c). On taking into consideration that fine-grained HAZ was already mixed with small grains after PWHT, the creep damage process can be divided into three regions.

Region I: Small creep void generates among small grains in fine-grained HAZ that has a tendency to cause dynamic recovery and dynamic crystallization. In other words, initial creep voids seem to be in an unstable microstructure including many small grains.

Region II: Creep strain concentrates around the initial creep void. The multiaxial stress also affects the initiation site of creep voids in HAZ in macroscopic investigation. As a result, very fine grains of less than $1\ \mu\text{m}$ develop along the random high angle grain boundaries (Fig. 3(a)) that are not subject to a K-S orientation relationship in the martensitic transformation. Sub-boundaries are formed inside the very fine grains by dynamic recovery and dynamic recrystallization.

Region III: Multiple creep voids are generated among very fine grains. In addition, creep voids combine inside the crystal and microcracks develop along the random high angle grain boundaries.

4. Conclusions

Microstructural changes during creep were examined by an interrupting creep test on welded joint in Mod.9Cr-1Mo steel under 60 MPa at 650°C . As a result, the creep damage sites were characterized by the formation of creep void and sub-boundary associated with an unstable microstructure as follows:

- The classification of grain boundaries using EBSD suggested that the sites of the generation of initial creep voids were on boundaries including the small grains derived from diffused α/γ transformation.
- Initial creep void formation is possible to promote preferential dynamic recovery and dynamic recrystallization around the high angle grain boundaries, followed by sub-boundary formation.

References

- [1] J. A. Francis, W. Mazur, and H. K. D. H. Bhadeshia, *Material Science and Technology*, 22 (2006) 1387–1395.
- [2] K. Yoshida and M. Yatomi, *Procedia Engineering*, 10 (2011) 490–495.
- [3] J. S. Lee, K. Maruyama, I. Nonaka, and T. Ito, “Mechanism of Type IV Failure in Weldment of a Mod. 9Cr-1Mo Steel,” Creep Deformation and Fracture, Design, and Life Extension (Materials Science & Technology 2005), Edited by R. S. Mishra, J. C. Earthman, S. V. Raj, and R. Viswanathan, TMS, Warrendale, (2005) 139–148.